Energy 70 (2014) 68–78

Contents lists available at ScienceDirect

Energy

journal homepage: www.elsevier.com/locate/energy

Pressurized gasification of torrefied woody biomass in a lab scale fluidized bed

C. Berrueco [a,*], J. Recari [b], B. Matas Güell [c], G. del Alamo [c]

[a] Bioenergy and Biofuels Area, Catalonia Institute for Energy Research, IREC, C/Marcel·lí Domingo, 2, Tarragona 43007 Spain
[b] Departament d'Enginyeria Química, Universitat Rovira i Virgili, Av. Països Catalans, 26, Tarragona 43007 Spain
[c] Department of Thermal Energy, SINTEF Energy Research, No-7465, Trondheim, Norway

A R T I C L E I N F O

Article history:
Received 22 June 2013
Received in revised form
15 March 2014
Accepted 21 March 2014
Available online 18 April 2014

Keywords:
Biomass
Torrefaction
Fluidised bed reactor
Steam/O_2 gasification
Biofuels

A B S T R A C T

This work reports experimental results concerning the influence of torrefaction level and pressure on product yields and composition during fluidized bed O_2/steam gasification of two different raw biomasses. The results show an increase in gas yield with pressure and torrefaction level for both types of biomass considered. Increasing pressure caused the produced gas composition to shift towards higher CH_4 and CO_2 content, while H_2 and CO levels decreased. The effect of the type of original biomass on gas composition was limited, and became less relevant as pressure and torrefaction level increased. The analysis of the tars produced during gasification also revealed that higher pressures led to the increase of tar yields. On the other hand, torrefaction level presented the opposite effect, with lower tar yields and lighter molecular weight distribution of tars as torrefaction level increased. Since torrefaction is being considered as a promising pretreatment technique for upgrading biomass to a higher quality solid fuel more suitable for the integration of gasification into biofuels production, the results from this study are relevant for evaluating the influence of the level of torrefaction on the performance of gasification under typical operating conditions in practical applications.

© 2014 Elsevier Ltd. All rights reserved.

1. Introduction

Nowadays, concerns about climate change effects and depletion of fossil fuels have drawn attention to find alternatives and more environmentally friendly ways of energy supply. Some of the major issues for fossil fuels are their non-renewable nature and the problems related to the release of pollutants (mainly CO_2, NO_x and SO_x) into the atmosphere [1], enhancing the global warming effect [2]. Despite that, fossil-derived fuels are the most common energy sources used in the world, reporting over 80% of the total energy consumption [3]. However, substantial efforts are being made on the development of alternative renewable energy sources that can replace the aforementioned fossil-derived fuels. In this context, biomass is reaching more positions and becoming one of the most widely used renewable energy sources. Biomass supplies about 15–20% of the total fuel use in the world [4], being currently the fourth largest resource of energy worldwide just after coal, oil and gas [5]. One of the main advantages associated with biomass is its conventional neutral CO_2 impact, when produced in a sustainable manner. Furthermore, among all renewable energies, biomass is the only storable and transportable source and the only renewable source of carbon, hydrogen and oxygen, which makes it a prime feedstock for production of multiple bio-based products within the next 20–30 years. In this scenario, biofuels, particularly for the aviation and heavy-duty trucks, have been recognized as one of the main pieces in the bioeconomy puzzle, as these transport sectors are not likely to be electrified in the coming decades and biofuels is thus the only near-medium term alternative to fossil-derived [6,7].

Despite the great potential of biomass, its use presents also a series of challenges. Two main limitations are the space needed to grow it and the expensive cost of transportation due to its low energy density [8]. Other drawbacks are high oxygen and water content, and hydrophilic properties [9].

A pretreatment stage prior to biomass conversion is needed in order to minimize some of the abovementioned drawbacks. In this context, torrefaction seems to be an effective option. Torrefaction is a thermochemical process that subjects the biomass at a temperature in the range of 200–320 °C in an inert atmosphere achieving

---

* Corresponding author. Tel.: +34 977 297 921; fax: +34 977 202 444.
E-mail addresses: cberrueco@irec.cat, cesar.berrueco@gmail.com (C. Berrueco).

http://dx.doi.org/10.1016/j.energy.2014.03.087
0360-5442/© 2014 Elsevier Ltd. All rights reserved.

a higher energy-dense product (almost moisture free) which is more feasible for transport. Besides, previous studies have shown other advantages of this technology, i.e., the fact that not only improves energetic value but also enhances feedstock homogeneity, grindability and hydrophobicity [10–14].

Another key aspect when evaluating the use of biomass as energy source is the conversion technology. Biofuels can be produced from a broad spectrum of conversion processes (biological, thermal and physical processes). Among the thermochemical conversion technologies, gasification is perceived as the most promising pathway to improve the efficiency in the use of biomass towards liquid fuels [8,15].

Biomass gasification has been exhaustively studied [8,16–19], particularly regarding the producer gas composition and heating value. The syngas composition can be influenced by several process parameters such as feedstock composition and particle size, gasification conditions, mainly temperature, equivalent ratio (ER), steam to biomass ratio and pressure [16,19], but also by the gasification reactor design.

With regards to temperature, Gil et al. [17] studied the gasification of pine chips with steam–oxygen mixtures in a fluidized bed gasifier varying the temperature from 780 to 890 °C. The study concluded that the increase of bed temperature leads to an increase in H_2 content, H_2/CO and CO/CO_2 ratios, together with higher thermal efficiencies of the process. Other studies on fluidized bed gasification of woody biomass [20–24] also have concluded that the introduction of steam was favourable to improve gas quality and that higher temperatures favoured both hydrogen production and gas yield. However, it was stated that gasification temperatures above 850 °C decreased the gas heating value, mainly due to the reduction of CO, CH_4 and C_2 hydrocarbons in the produced gas.

Mayerhofer et al. [25] studied the gasification of wood pellets in a bubbling fluidized bed (BFB) varying several operating conditions (temperature, pressure and steam to biomass ratio (S/B)). The results showed that high temperatures (750–840 °C) promoted the formation of H_2, while CH_4 and CO_2 content decreased. Additionally, higher S/B ratios shifted the gas composition to higher concentrations of H_2 and CO_2 and lower contents of CO and CH_4 in the produced gas, which can be explained qualitatively with the enhanced water gas shift reaction. Lastly, pressure had a significant effect on the effluent gas composition [25]. For comparable temperatures and S/B, and increase in gasification pressure led to higher CH_4 content due to the enhancement of the methanation reaction at high pressures, together with a slight increase in H_2 content, and lower CO/CO_2 ratios.

The bibliographic revision denotes that although gasification is influenced by several other parameters, the two principal studied parameters have been temperature and ER. This fact evidences a lack of studies related to the effect of pressure and biomass feedstock properties (influenced by (i) feedstock nature and (ii) thermal pretreatments such as torrefaction level) on syngas composition.

The goal of this paper is to study the influence of pressure and biomass composition (by the gasification of two different biomasses at three different torrefaction levels: raw biomass, lightly torrefied and significantly torrefied), on product yields and composition during fluidized bed O_2/steam gasification. The obtained results will allow the evaluation of gasification performance in order to determine optimal operation conditions. Notice that the information here presented has been obtained in a lab scale gasifier, and although the main trends and conclusions of this study can be useful to give insight to the gasification of torrefied biomass, the actual numbers could be different in an industrial scale gasifier.

2. Experimental

2.1. Sample characterization and preparation

Norwegian spruce and Norwegian forest residues (mainly tops and branches), hereby referred as VW and GROT, respectively, were obtained from local sources in Trondheim, Norway. The original biomasses were treated at two different torrefaction levels: Lightly torrefied LT (final torrefaction temperature of 225 °C) and significantly torrefied ST (final torrefaction temperature of 275 °C). The raw samples and torrefied products were sieved to a particle size range of 250–500 μm. The proximate and ultimate analyses were carried out using a LECO Thermogravimetric analyzer (TGA 701) and a LECO TruSpec CHN–S–O analyser, respectively. The proximate analyses of all samples were conducted following the ASTM D7582 standard test method for moisture, volatile matter, and fixed carbon determination. The results together with the lower heating values (LHVs) are included in Table 1. The determination of the heating value of the samples was performed in an isoperibol LECO Automatic calorimetric bomb (AC600), according to the ASTM D5865-07standard test method. After each measure the bomb was washed out with a 0.2 M KOH solution to recover sulphur (H_2SO_4), halogens (HCl, HF, HBr) and phosphorous (H_3PO_4), which were measured afterwards by ionic chromatography (Dionex ACS 1100) according to the EN-15408:2011 standard method.

2.2. Setup and procedure for torrefaction

Torrefaction experiments were performed using a bench-scale continuous reactor consisting of four independent horizontal conveyors positioned in parallel from top to bottom. Each conveyor consisted of a horizontal pipe (i.d.: 100 mm) with a screw conveyor that allowed a precise control of temperature and residence time of the different stages. Drying, heating and cooling conveyors had a length of 700 mm, whereas the torrefaction conveyor was 1000 mm long. The reactor, capable of operating at temperatures of up to 300 °C, had a capacity of 0.2–7.0 kg/h of biomass in size range of 1–25 mm. The feedstocks were first ground and afterwards compressed to produce pellets of 6 mm diameter without adding binders. These pellets were fed from the storage hopper to the first conveyor by a feeding screw, after that the fed material passed through the screw conveyors for drying, heating to torrefaction temperature, torrefaction and cooling and finally left by gravity to a collecting vessel. Notice that the material was transferred between conveyors using pneumatically controlled sliding valves. The conveyors were temperature controlled using electrical heating elements with the exception of the last one, where torrefied material was cooled using a water jacket. In order to ensure inert conditions and remove the volatiles, each part of the reactor (including the hopper and the collecting container) was purged with a nitrogen flow of about 8 NL/min.

Feeder and screws were driven by individual motors allowing for basically independent setting of mass flow (feeder setting) and residence time (screw setting). However, since the filling degree of the screws was limited, the settings were not fully independent from each other.

2.3. Fluidized bed gasifier

Gasification experiments were conducted on a laboratory-scale pressurized fluidized bed reactor (PID Eng & Tech, Spain), schematized in Fig. 1. The experimental rig was equipped with a

Table 1
Main characteristics of feedstocks.

		VW	VW-LT	VW-ST	GROT	GROT-LT	GROT-ST
Proximate analysis[a] (wt.%)	Moisture	5.03 ± 0.01	3.45 ± 0.01	3.79 ± 0.01	6.26 ± 0.03	4.79 ± 0.01	4.17 ± 0.01
	Volatiles	77.15 ± 0.12	77.44 ± 0.04	72.34 ± 0.06	70.06 ± 0.12	68.91 ± 0.12	61.63 ± 0.11
	Fixed carbon	17.46 ± 0.12	18.70 ± 0.05	23.41 ± 0.05	21.50 ± 0.18	24.13 ± 0.17	31.47 ± 0.11
	Ash	0.36 ± 0.02	0.42 ± 0.01	0.46 ± 0.01	2.19 ± 0.03	2.27 ± 0.05	2.73 ± 0.02
Ultimate analysis[a] (wt.%)	C	47.20 ± 0.17	48.86 ± 0.48	52.72 ± 0.29	47.58 ± 0.28	51.13 ± 0.46	56.84 ± 0.08
	H	6.21 ± 0.10	6.08 ± 0.13	5.88 ± 0.11	6.10 ± 0.08	5.93 ± 0.09	5.51 ± 0.10
	O	46.18 ± 0.30	44.57 ± 0.55	40.86 ± 0.40	43.62 ± 0.30	40.26 ± 0.50	34.29 ± 0.20
	N	0.02 ± 0.02	0.05 ± 0.02	0.06 ± 0.02	0.48 ± 0.02	0.49 ± 0.01	0.61 ± 0.02
	S	0.03 ± 0.002	0.03 ± 0.002	0.03 ± 0.002	0.07 ± 0.002	0.07 ± 0.005	0.06 ± 0.004
	F	>0.0015	>0.0015	>0.0015	>0.0015	0.0021 ± 0.0001	0.051 ± 0.0011
	Cl	0.0021 ± 0.0001	0.0022 ± 0.0001	0.0021 ± 0.0003	0.0545 ± 0.0012	0.0220 ± 0.0006	0.0131 ± 0.0007
	P	0.0018 ± 0.0007	0.0019 ± 0.0007	0.0021 ± 0.0005	0.0054 ± 0.0009	0.0156 ± 0.0011	0.0216 ± 0.0028
LHV [MJ/kg][a]		17.74 ± 0.09	18.26 ± 0.04	19.80 ± 0.03	18.22 ± 0.04	19.30 ± 0.03	21.74 ± 0.02

[a] "As received" basis.

complete control system including, flow control, feeding system control, pressure control, together with several temperature measurement points, temperature control inside the fluidized bed and freeboard. The body of the reactor consisted in a 404-mm-long (23.8 mm internal diameter) Hastelloy C pipe, capable of operating at pressures of up to 20 bar and temperatures of up to 900 °C. The solid fuel was continuously fed into the bed by means of a screw feeder, at feed rates from 0.2 to 5 g/min. Water flow was pumped into the steam generator using a GILSON HPLC pump (0–5 ml/min range) before it was injected in the reactor. The product gas went through a cyclone and hot filter (10 μm) to remove entrained solids. After that the gas was cooled in a condenser (5 °C) and an ice-salt tar trap (−10 °C). An additional trap, packed with stainless steel mesh, was installed at the outlet to ensure efficient trapping of the tars in the form of aerosol droplets. The gas composition and flow were measured by means of an online micro GC (Agilent 490) and a Bronkhorst High-Tech flowmeter, respectively.

The fluidized bed reactor is commonly used for biomass gasification, and additionally it presents a series of advantages for its operation at lab scale. It allows a fast heating of the biomass particles and a quite precise temperature control in the fluidized bed (where the main char gasification reactions take place). On the other hand, the gas and tar products keep reacting along the freeboard zone with an approximately linear decay of temperature of about 50 °C.

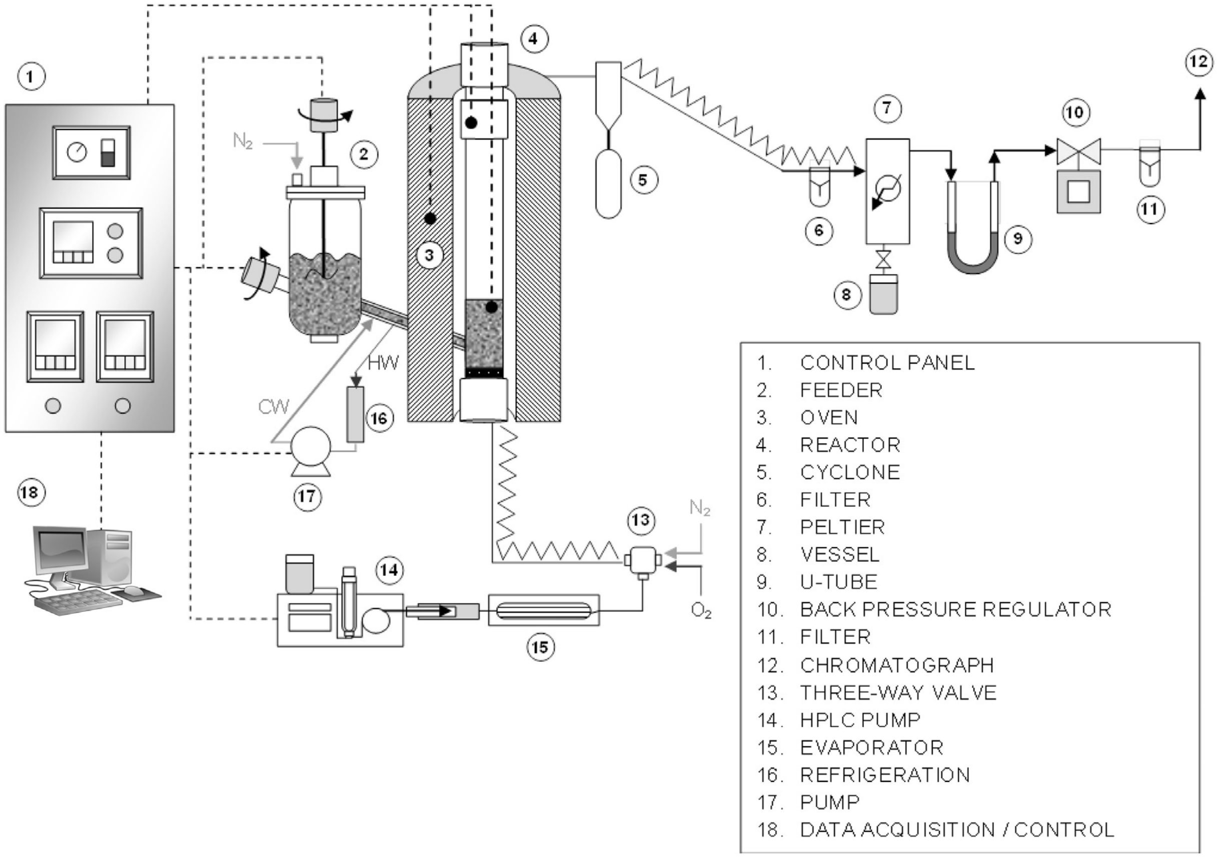

Fig. 1. Flow sheet of the bench-scale fluidized bed reactor.

2.3.1. Experimental procedure

The required amount of feedstock was placed in the hopper, and the agitation and feeding screws were set to the desired feed rate. The reactor was filled with 50 g of sand (silica with particle size 150–200 μm), fluidized on a stream of N_2 (Praxair, Inc.) during the heating period up to the experiment temperature. During the heating period, the online micro GC was calibrated, using a gas calibration mixture. Once the temperature was reached, the gas flow was switched from N_2 to O_2 (Praxair, Inc.) and the system was pressurized to the experimental final conditions. As soon as the system was stable, the solid and water feeds were switched on. A constant gas composition was reached after about 5 min of starting the feeding (these are the gas compositions reported in this study). The experiment length was about 60 min for all the performed tests.

At the end of the experiment, tars were recovered by washing the tar trap with a mixture of $CHCl_3$:MeOH (4:1 vol:vol). The solvent was removed by rotavap and then by purging with N_2 until the tar was completely dry. The unconverted solid particles remaining in the bed, filter and cyclone were also collected after the completion of the test for characterisation.

The gasification was performed under O_2/steam atmosphere, with an equivalence ratio (ER) around 0.23 and a steam/biomass ratio of about 1.6 and three different pressure levels (0.1, 0.5 and 1.0 MPa). The operation flows provided a fluidizing gas velocity six to seven times the minimum fluidization velocity (U_{mf}), corresponding to gas residence times in the reactor of 2.0–2.4 s. Mass balances were calculated taking into account the mass of gases produced (gas balance) and the weight of tar and unconverted solid particles. Adequate mass balance closures ($\geq$95%) were obtained for all the conducted experiments.

2.4. Gas and tar analysis

An online micro GC (Agilent 490) was used to quantify the major components in the fuel gas during the experiments. The chromatograph configuration included three different channels: Channel 1, equipped with a 10 m MS5A (Molecular Sieve 5A), running on argon as carrier gas for the analysis of permanent gases other than carbon dioxide (H_2, O_2, N_2, CO and CH_4). Channel 2 was equipped with a 10 m PoraPlotQ and used helium as carried gas, allowing the separation of CO_2 and saturated and unsaturated C_1–C_3 hydrocarbons. The C_3–C_5 hydrocarbons were analysed on the third channel (also using helium as carrier gas) with a 10 m Al_2O_3 column. Detection was carried out by means of micro-machined thermal conductivity detectors (μTCD), included in each channel.

An Agilent Technologies 1100 Series HPLC system was used to perform the size exclusion analysis of the obtained tars. Three (300 mm long, 7.5 mm i.d.) polystyrene/polydivinylbenzene-packed columns (PL Gel 10^4 Å 5 μm, PL Gel 500 Å 5 μm and PL Gel 50 Å 5 μm) were used (Polymer Laboratories, Church Stretton, UK). The system was operated at 80 °C and a flow rate of 0.5 mL/min. *N*-methyl 2-pyrrolidinone (NMP) was used as the mobile phase. Detection was carried out using a diode array UV-absorbance detector. As NMP is opaque at 254 nm, detection of standard compounds and samples was performed at 270, 300, 350 and 370 nm, where NMP is partially transparent. The results obtained at 300 nm were considered representative of the main trends observed at all wavelengths; only those results will be shown and discussed. System calibration was carried out using two sets of standards, PS standards calibration was applied to the 30–52 min time range, while polycyclic aromatic hydrocarbon (PAH) compounds calibration was used in the 52–62 min region [26–28].

The calibration used to convert elution time to mass estimates was as follows:

Elution time	Calibration equation	Basis
<27.5 min	>200,000 u average mass (Mn)	
27.5–47.5 min	$\log(MM) = 8.6855 - 0.1232 \times (\text{time})$	Polystyrene (PS)
47.5–60.0 min	$\log(MM) = 6.0797 - 0.0682 \times (\text{time})$	PS + PAH std's
>60.0 min	Approximately 100 u	PAH std's

In order to compare structural features of the tar compounds Fourier transform infrared (FT-IR) spectroscopy was carried out in a Bruker Vertex 70 spectrometer equipped with Platinum diamond ATR unit. Tar spectra were collected at room temperature in the range 400–4000 cm^{-1} by co-addition of 32 scans at a nominal resolution of 4 cm^{-1}, taking the spectrum of the empty cell at ambient conditions as the background.

3. Results and discussion

3.1. Fuel characterization of the raw and torrefied materials

As stated in the experimental section, torrefaction was performed using a bench-scale continuous reactor. Both raw biomasses (VW and GROT) were torrefied at two different torrefaction levels (LT (Lightly Torrefied) and ST (Significantly Torrefied)), giving a total of six different feedstocks. The torrefaction temperatures were selected based on previous studies [13,29–31]. In particular Park et al. [30], reported the highest energy yield for samples torrefied at 275 °C when processing woody biomass under torrefaction and low-temperature carbonization conditions (250–375 °C).

Table 1 presents the main characteristics of the six studied feedstocks, in terms of elemental analysis and heating value.

3.1.1. Proximate analysis

The obtained results indicate a general increase in fixed carbon content and a decrease in moisture and volatile content as the degree of torrefaction conditions intensified, being this effect independent on the biomass nature. Another aspect worth noting is that, independently on the biomass, the most relevant changes in fixed carbon and volatiles took place in the interval from lightly torrefied (LT) to significantly torrefied (ST) with variations of about 5–7% versus 1–2% in the interval raw to LT. On the other hand, moisture decrease was more noticeable in the interval from raw to LT (around 1.5%), and much less important from LT to ST. These results revealed that the main changes in the interval from raw to Lightly Torrefied (LT) materials were related to the decrease in moisture content, whereas variations in fixed carbon and volatile content were more significant in the temperature range from 225 to 275 °C (LT to ST).

3.1.2. Ultimate analysis

Table 1 also presents the ultimate analysis of the feedstocks. Comparing both raw biomasses, GROT presented lower levels of hydrogen and oxygen, together with higher levels of carbon and other minor components (N, S, Cl and P), usually related to contaminants emission. The ash content of GROT sample (2.2%) was about six times larger than the one observed for VW (0.4%). This fact is directly related to the nature of GROT, this biomass consists in forest residues that contain significant larger amounts of inorganics as compared to cleaner VW.

The torrefaction process resulted in an increase in carbon, nitrogen and ash contents whereas the hydrogen and oxygen levels decreased. Sulphur content remained nearly constant.

The obtained results are in agreement with previous studies that show that the main changes derived from torrefaction process on the properties of the solid product are related to the removal of oxygen from the raw biomass [32,33]. In particular, the chemical changes due to torrefaction involve decomposition of hemicelluloses (160–200 °C) and partial depolymerisation of cellulose (240–350 °C) and lignin (280–500 °C) [29,30]. Water is a major product released during the process, firstly during drying when moisture evaporates and secondly during dehydration reactions between organic molecules [31]. As a result, the torrefied materials become more coal like and energy dense than the original biomass [9], enhancing its fuel properties for gasification processes [34].

3.1.3. *O/C and H/C ratios*

The torrefaction effect on oxygen and hydrogen content is further illustrated in Fig. 2 (Van Krevelen diagram). The O/C and H/C ratios were 0.73 and 1.58, respectively, for raw VW and 0.69 and 1.54 for raw GROT. These ratios decreased only marginally at a torrefaction temperature of 225 °C for both materials. However, a significant decrease was observed when torrefaction temperature increased up to the ST conditions. At 275 °C, the O/C and H/C ratios decreased up to 0.58 and 1.34 for VW and 0.45 and 1.16 for GROT, respectively, in line with the results from the proximate analysis discussed above.

3.1.4. *Heating value*

The loss of moisture and light oxygenated compounds also resulted in an improvement of feedstock heating value [11,35]. This effect is clearly observed in Table 1. Raw VW and GROT presented LHVs of 13.9 and 14.4 MJ/kg, respectively. The energy increase of the torrefied VW was similar to the one presented in previous studies for other wood samples. In particular the increase in the HHV of leucaena samples treated at 225 and 275 °C with 30 min of holdup time were reported to be 4.4% and 12.3% [36]. On the other hand, GROT samples exhibited an LHV increase similar to those reported for logging residue chips and pine chips under the same pretreatment conditions: 5.3% and 17.2% and 5.5% and 18.2%, respectively [37]. The results reflect the differences between the feedstocks, showing the higher reactivity of GROT as compared to VW under torrefaction conditions.

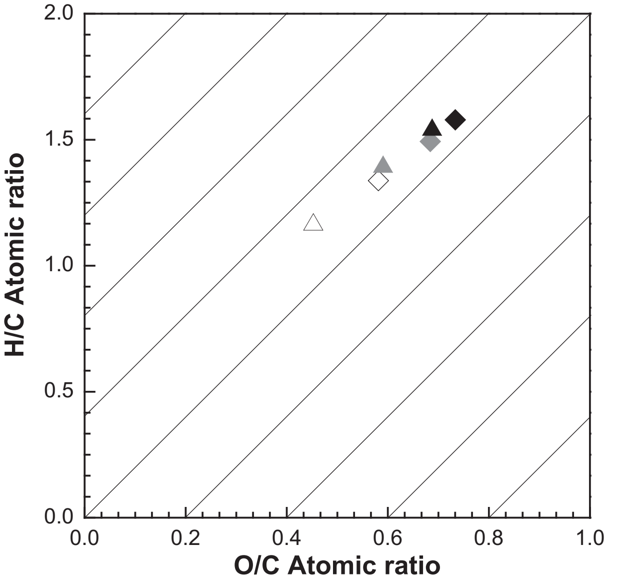

Fig. 2. Van Krevelen diagram for the raw and torrefied samples [◆ VW, ◆ VW-LT, ◇ VW-ST, ▲ GROT, ▲ GROT-LT, △ GROT-ST].

3.2. *Bench-scale fluidized bed gasification of torrefied biomass*

3.2.1. *Product yields*

Table 2 shows the results obtained in terms of variation of gas, tar and char yields during the experiments under different experimental conditions. These yields are calculated as the percentage of mass of compound per mass of dry biomass. As a result of using this basis the sum of gas, tar and char yields results above 100%, since products are formed due to the reaction with the gasification agents (O_2 and steam).

3.2.1.1. Effect of torrefaction level. The obtained results showed an increase in gas yield as torrefaction level increased. The cited rise was more relevant for GROT materials – experiments 10 to 18 – (with increases in the order of 6–11% comparing gasification gas yield of raw GROT and GROT-ST), than those obtained when VW materials- experiments 1 to 9- were gasified (3.2–6.9%). Additionally, tar yield decreased for more severe torrefaction conditions. For instance, tar yield varied from 1.1 to 0.2% when GROT and GROT-ST (experiments 10 and 16) were gasified at atmospheric pressure. This decrease was slightly lower in the case of VW and VW-ST, although tar production was always lower for this particular biomass and its torrefied products. Char yield presented an increase for both studied biomasses as the torrefaction level increased, but only at the lowest tested pressure (0.1 MPa). This increase was almost double for GROT (experiments 10, 13 and 16) in comparison to VW materials (experiments 1, 4 and 7). However the effect of torrefaction level on char yield at higher pressures was not evident (0.5 and 1.0 MPa). Different trends were observed depending on the torrefaction level and original feedstock (VW or GROT). A possible explanation for this uncertain trend is the competition between two mechanisms, on the one hand, the more relevant role of char gasification for more torrefied materials (that increases with pressure), and the effect of tar repolymerization to produce char [25,38,39].

3.2.1.2. Effect of pressure. Pressure presented a clear effect on gas yield, which increased in the whole range of torrefaction level and for both biomasses. The results showed a slightly higher gas yield for the experiments carried out using VW-derived feedstocks as compared with the GROT-derived samples. Additionally, the effect of pressure on gas yield rise differed for both biomasses. The increase in gas yield with pressure was similar for the original biomasses, however a sharper increase with pressure was observed for GROT torrefied materials in comparison to VW materials. Thus, the increase in gas yield for GROT-LT and ST in the interval from 0.1 to 0.5 MPa (experiments 14 and 17) was about 9.5% in comparison to the 3.8 and 2.5% obtained for VW-LT and ST, respectively (experiments 5 and 8). Tar yield increased with pressure for both biomasses, with GROT and its torrefied materials always yielding higher levels of tar than the correspondent VW materials. The tar yield rise with pressure was quite remarkable, and appeared to be more pronounced in the pressure interval from 0.1 to 0.5 MPa. Tar evolution with pressure was probably related to the formation of PAH compounds, more relevant at higher pressure [25]. Regarding char yield evolution, in general it decreased with gasification pressure (the decrease differed for the different levels of torrefaction and original feedstock). As indicated above, the two competing mechanisms can explain char evolution, and increasing pressure would favour char gasification reactions [25,38,39].

3.2.2. *Gas composition*

The main components of the gas were H_2 (30–40%$_{db}$ vol.), CO_2 (30–37%$_{db}$ vol.), CO (18–24%$_{db}$ vol.) and CH_4 (4–12%$_{db}$ vol.), whereas O_2, C_2H_4, C_2H_6 and C_3H_8 appeared in lower concentrations.

Table 2
Experimental conditions and product yields for the gasification of the six biomass samples at 850 °C.

Run number	Feedstock	Pressure (MPa)	ER	Ratio g H_2O/g dry biomass	Yield (g/100 g dry biomass)		
					Gas	Tar	Char
1	VW	0.1	0.22	1.6	133.6 ± 0.3	0.52 ± 0.03	2.06 ± 0.05
2	VW	0.5	0.24	1.7	139.4 ± 0.5	0.64 ± 0.02	2.46 ± 0.06
3	VW	1.0	0.24	1.7	147.3 ± 0.3	1.58 ± 0.05	2.10 ± 0.04
4	VW-LT	0.1	0.23	1.6	138.3 ± 0.1	0.18 ± 0.02	2.80 ± 0.06
5	VW-LT	0.5	0.23	1.6	142.1 ± 0.4	0.98 ± 0.02	2.18 ± 0.05
6	VW-LT	1.0	0.22	1.6	146.4 ± 0.3	1.31 ± 0.03	2.59 ± 0.04
7	VW-ST	0.1	0.22	1.5	140.4 ± 0.2	0.11 ± 0.01	3.41 ± 0.03
8	VW-ST	0.5	0.24	1.7	142.9 ± 0.2	0.64 ± 0.02	2.28 ± 0.09
9	VW-ST	1.0	0.23	1.6	150.5 ± 0.5	0.67 ± 0.03	1.93 ± 0.04
10	GROT	0.1	0.23	1.6	130.3 ± 0.5	1.08 ± 0.02	3.10 ± 0.05
11	GROT	0.5	0.23	1.6	137.2 ± 0.3	1.75 ± 0.03	2.68 ± 0.05
12	GROT	1.0	0.23	1.5	143.4 ± 0.4	1.95 ± 0.06	2.40 ± 0.07
13	GROT-LT	0.1	0.22	1.6	131.8 ± 0.3	0.50 ± 0.01	4.13 ± 0.10
14	GROT-LT	0.5	0.21	1.6	141.4 ± 0.2	1.18 ± 0.02	2.24 ± 0.07
15	GROT-LT	1.0	0.23	1.7	144.0 ± 0.5	1.54 ± 0.02	2.22 ± 0.05
16	GROT-ST	0.1	0.22	1.6	138.5 ± 0.2	0.19 ± 0.01	5.37 ± 0.08
17	GROT-ST	0.5	0.22	1.6	148.1 ± 0.4	0.70 ± 0.02	4.49 ± 0.10
18	GROT-ST	1.0	0.22	1.7	149.1 ± 0.2	1.03 ± 0.01	4.39 ± 0.09

GROT: forest residues; VW: virgin wood; LT: lightly torrefied; and ST: significantly torrefied.

The evolution of the gas composition under different experimental conditions can be explained taking into account the initial devolatilization of the biomass, which forms light gases and primary tars, followed by their subsequent conversion through steam reforming, oxidation, methanation and water gas shift [3,40]:

Note that, in order to compare the main trends on gas product evolution under the different experimental conditions, the results are presented as weight of gas product by 100 g of dry biomass (Fig. 3 (VW) and Fig. 4 (GROT)).

3.2.2.1. Effect of torrefaction level.

The torrefaction level presented a positive effect on hydrogen yield, the results showed an increase in hydrogen yield of about 0.6% for VW-LT in comparison with original VW for all tested pressures, whereas the increment was more important in the case of GROT (around 1.3, 1.4 and 0.9% for 0.1, 0.5 and 1.0 MPa, respectively).

The influence of torrefaction level on the rest of permanent gases was not that evident. It can be observed a reduction in both methane yield and concentration in the fuel gas for the highest torrefaction level and pressure, although this trend varied under other experimental conditions (i.e. GROT at 0.1 MPa). Influence of torrefaction level on CO and CO_2 was again limited, although a slight increase in CO and CO_2 yields could be depicted from the plots.

The significant increase of H_2 and the simultaneous increase of CO, CO_2 together with the reduction of the hydrocarbons in the product gas can be explained by evaluating the changes in feedstock composition with torrefaction. The higher the torrefaction level, the lower the contribution of devolatilization to the product gas formation, while char gasification would play a more relevant role in the process [39]. The main gas products by char gasification are H_2 and CO, so in theory their production would be favoured by more torrefied feedstocks. The lower influence of torrefaction on the CO yields is directly related to the presence of O_2 and the equilibrium CO—CO_2. Additionally, it is worth noting that the main differences between the original biomasses (VW and GROT) and its correspondent torrefied materials were observed at atmospheric pressure (0.1 MPa). The differences became less relevant as pressure and torrefaction level increased (more severe conditions).

3.2.2.2. Effect of pressure.

Among the observed trends, H_2 yield decreased as pressure increased for both studied biomasses. This drop with gasification pressure can be explained taking into account the gasification reactions [41]. At high pressure the chemical equilibrium of the hydrogen production reactions (heterogeneous water gas reaction, steam reforming reaction and hydrogenation reaction) is shifted to the reactant side.

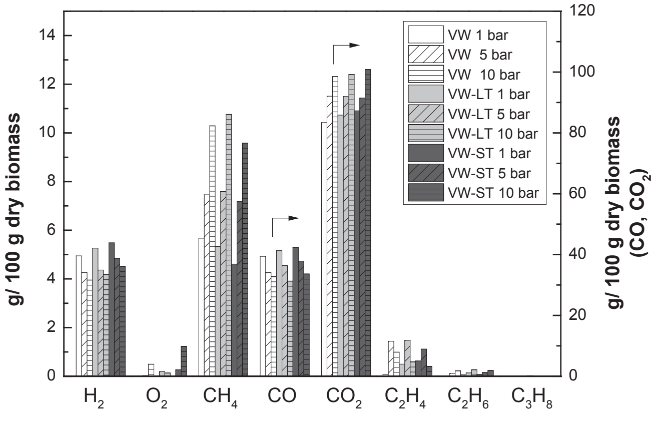

Fig. 3. Effect of pressure and torrefied level on gas yields (VW). Temperature 850 °C, ER: 0.23, H_2O/Biomass: 1.6.

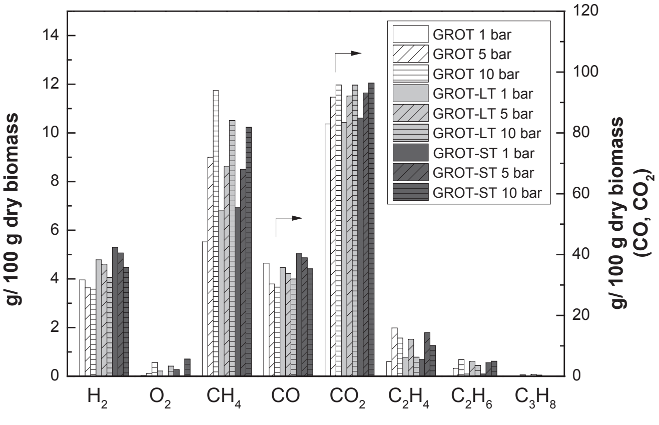

Fig. 4. Effect of pressure and torrefied level on gas yields (GROT). Temperature 850 °C, ER: 0.23, H_2O/Biomass: 1.6.

Increasing pressure provokes also an enrichment of the producer gas with methane. This trend can be explained by the fact that pressure favours the methanation reaction, especially at moderate temperatures [42]. For instance methane yield in experiments using VW-derived samples as feedstock increased from 5.7, 5.3 and 4.6% at 0.1 MPa to 7.5, 7.6 and 7.2% at 0.5 MPa and 10.3, 10.8 and 9.6% at 1.0 MPa, respectively. Experiments using GROT and its torrefied materials as feedstock showed similar trends, however the increase in methane yield was lower when GROT-LT and GROT-ST were used as feedstock.

Regarding the evolution of CO and CO_2 yields with pressure, these compounds presented an inverse trend, mainly due to the Boudouard reaction [25,42]. Formation of CO is favoured at low pressures within the temperature and ER range used in the present study, whereas CO_2 formation is promoted at higher pressures (above 0.3 MPa). Comparing the results obtained for both biomasses, higher CO yields were obtained for gasification experiments of VW and its torrefied materials in all the range of experimental conditions, with the exception of higher pressures and torrefaction. Additionally, the drop in CO yield as pressure increased was more intense for the VW materials. CO_2 yields presented quite similar values, the most relevant differences appeared at high pressure (1.0 MPa) and torrefaction level (CO_2 yields: 99.2 and 100.8% for VW-LT and VW-ST and 95.7 and 96.4 for GROT-LT and GROT-ST, respectively).

C_2 and C_3 hydrocarbons appeared in lower level than the rest of the permanent gases for the different feedstocks in all the studied range of pressure. However, some changes were consistently observed on C_2H_4 and C_2H_6 yields. In all cases, these compounds presented a maximum yield at 0.5 MPa, with a decrease at higher pressure. This trend may be related with the mechanisms of formation of secondary tars, which are relevant under the studied conditions (850 °C and high pressure) [25,38]. Several mechanisms have been proposed to explain the growth of PAH compounds, some of them indicate the role of C_2 and C_3 hydrocarbons in the process [43–45].

3.2.3. *Tar characterization*

This section summarizes the evolution of tar content in the produced gas, together with a preliminary characterization of the tars in terms of molecular weight distribution and chemical structure.

3.2.3.1. Tar content. The results of tar content in the dry produced gas (expressed as g/Nm^3) appear displayed in Figs. 5 and 6 for the experiments performed with VW- and GROT-derived feedstocks, respectively.

The data showed an increase in tar content as pressure increased in all the studied range and for both biomasses. This increase was, in general, more marked in the interval from 0.1 to 0.5 MPa (especially for the significantly torrefied biomasses). The pressure effect on primary tars causes a greater resistance exerted by the sweeping gas on the escaping volatiles. This causes an increase in the material residence time resulting in repolymerization reactions and carbon reincorporation into the forming char, and a decrease on tar yields [18]. Additionally, the pressure also has an effect on the evolution of the secondary tar reactions along the reactor and freeboard. This parameter probably enhances the tar polymerization reactions towards polycyclic aromatic hydrocarbon (PAH) compounds [25]. Decrease of C_2 and C_3 hydrocarbons in gas phase at high pressure also supported this hypothesis, as these compounds can be involved on PAH growth mechanisms [43–45].

Additionally, the results evidence that torrefaction level affected the tar content in the produced gas. The tar content decreased as torrefaction level increased, being this effect more relevant for GROT-derived materials in comparison to VW-derived materials. It is worth noting that tar content in the fuel gas was higher for GROT and GROT torrefied materials, in comparison with VW, although this difference diminished with the torrefaction level. The effect of torrefaction level on tar content can be explained taking into account the changes in feedstock composition with torrefaction. The higher the torrefaction level, the lower the volatile content of the feedstock, parameter directly related to tar evolution.

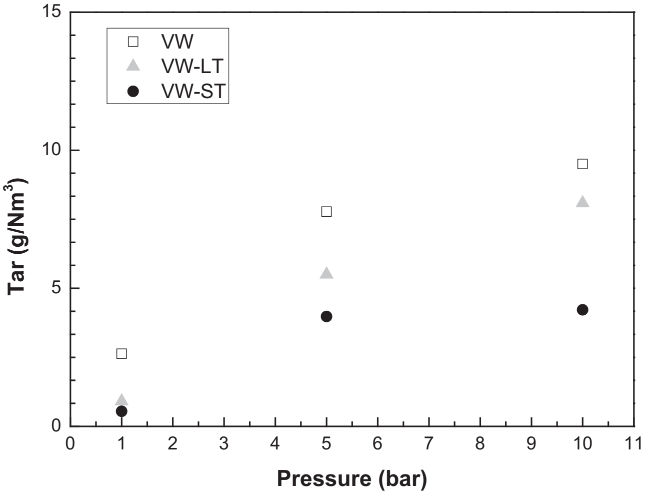

Fig. 5. Effect of pressure and torrefied level on tar content (VW). Temperature 850 °C, ER: 0.23, H_2O/Biomass: 1.6.

3.2.3.2. Molecular weight distribution (SEC). The examination of the molecular weight distribution of biomass tars was carried out using the SEC system described in Section 2. Figs. 7 and 8 present some examples of the molecular weight distribution of tars obtained at different pressures and levels of torrefaction for VW and GROT, respectively. All the curves showed bimodal distributions of signal in all the cases, the earliest eluting peak corresponds to the material of molecular size unable to penetrate the porosity of the column packing, and referred to as “excluded” from the column porosity. The second eluting peak corresponds to the material able to

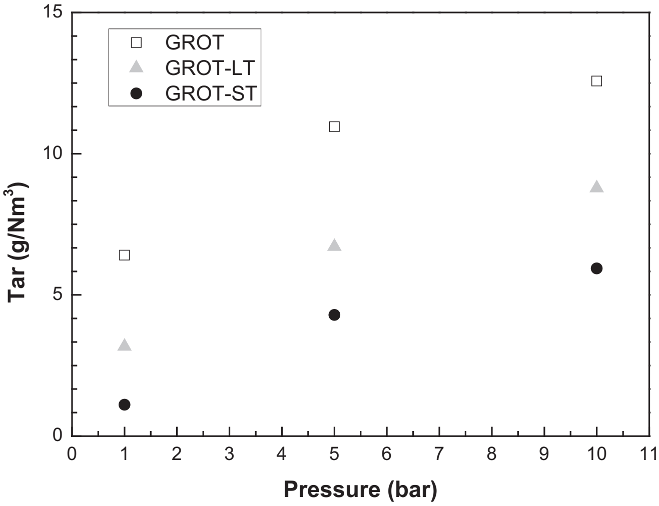

Fig. 6. Effect of pressure and torrefied level on tar content (GROT). Temperature 850 °C, ER: 0.23, H_2O/Biomass: 1.6.

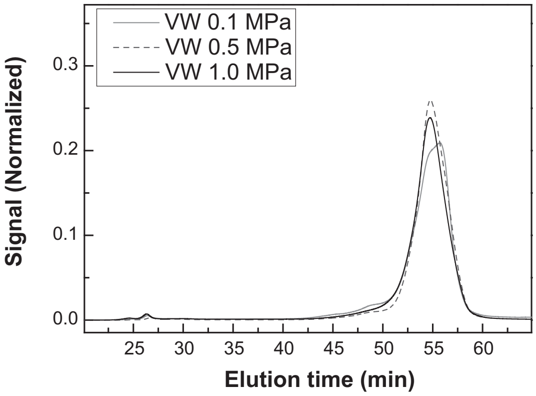

Fig. 7. Size exclusion analysis of VW tars obtained in an FBR, influence of pressure and torrefaction level.

penetrate the porosity of the column packing. The exclusion limit of the column, defined according to the standards of polystyrene behaviour, is about 200,000 u. However, molecular conformation is considered to be the factor that causes molecules to become excluded from the column porosity rather than the molecular weight [26,27]. Estimates of molecular masses can be calculated from a mass calibration based on the elution times of polystyrene (PS) standards and polycyclic aromatic hydrocarbon (PAH) standards.

Comparing the results of the SEC analysis of the tars obtained from GROT at various pressures and torrefaction levels (Fig. 8), it can be noticed that they presented similar MW distributions, although several trends can be extracted. The tars obtained at higher pressures presented slightly heavier molecular weight distribution curves (particularly remarkable for GROT-ST). The tars obtained when GROT-ST was gasified at 0.1, 0.5 and 1.0 MPa showed a distribution shifted to higher MWs with maxima at 56.3, 56.1 and 54.5 min, which correspond to a mass of about 175, 180 and 230 u, respectively. The lift-off of the retained peak appeared around 44.5, 41.7 and 39.9 min, corresponding to masses of 1600, 3500 and 5900 u, respectively. This fact agrees with the increase in tar yield observed at higher pressures, probably related to polymerization towards heavier PAH compounds [25].

On the other hand, the torrefaction level presented an opposite trend, the obtained results showed decreasing molecular weight distribution of tars in the order: raw biomass > LT > ST. For instance the tars obtained during the gasification of GROT, GROT-LT and GROT-ST at 0.1 MPa showed lift-off around 40.4, 41.3 and 44.5 min respectively, which correspond to a mass of about 5100, 3950 and 1600 u taking into account the calibration, and a maxima intensity that corresponded to 220, 190 and 175 u, respectively. This effect declined as the gasification pressure increased, in particular at the highest evaluated pressure (1.0 MPa), the tars obtained under these conditions presented analogous molecular weight distributions. These results are comparable to those obtained for VW (Fig. 7), however, in this case, the tars obtained at pressures higher than 0.1 MPa presented resembling molecular weight distributions.

3.2.3.3. FT-IR analysis. Figs. 9 and 10 show the FT-IR spectra of the tars obtained in the fluidized bed reactor at different pressures and torrefaction levels. The tar spectra showed in all the cases absorption bands corresponding to aromatic structures at 3050, 1600, 870, 813 and 750 cm^{-1} and aliphatic structures at 2960, 2922, 2855, 1352 and 1379 cm^{-1}. The bands in the region 900–700 cm^{-1} are usually assigned to the out-of-plane bending of aromatic CH groups. The bands in the region 1630–1470 cm^{-1} are assigned to the stretching of aromatic C=C groups and bands at 3050 and 3016 cm^{-1} to the stretching of aromatic C–H groups. The bands in the 2968–2864 and 1444–1377 cm^{-1} regions are due to the stretching and bending modes of saturated aliphatic hydrocarbons (C–H). Additionally, peaks appearing at 1100–1300 and 1700 cm^{-1} are assigned to phenoxyl and ether stretching and carbonyl groups, respectively.

For both feedstock materials, the results showed a decrease in the aliphatic band (2990 cm^{-1}) together with an increase in the signal of the different aromatic bands as pressure increases. The signal in the oxygenated functionalities decreased when pressure increased (more relevant in the range 0.1–0.5 MPa). These results indicate that an increase in pressure favours the formation of oxygen-poor polyaromatic compounds. Among the oxygen

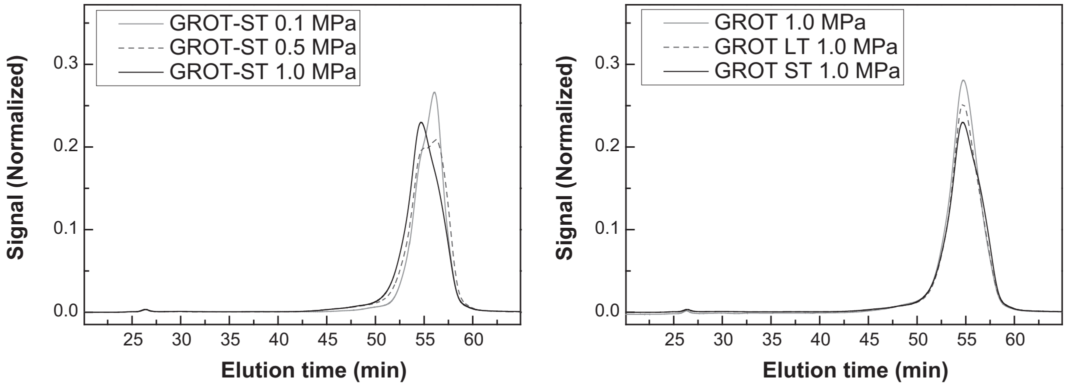

Fig. 8. Size exclusion analysis of GROT tars obtained in an FBR, influence of pressure and torrefaction level.

functional groups present in the tars, C=O structures (broad band at 1715–1650 cm^{-1}), methoxyl groups (1265 cm^{-1}) and C–O bands (1035 cm^{-1}) could be detected. The signal in the oxygenated functionalities was also lower for the most torrefied samples (ST) as compared to the raw material, which is in good agreement with the composition of the initial feedstock.

3.2.4. *Effect of experimental parameters on gasification performance*

This section gathers a series of parameters that allow, together with the information related to syngas composition and tar content presented beforehand, the assessment of the gasification performance. It is important to notice that these parameters are presented as qualitative information and are not directly applicable to industrial gasifiers. Two aspects are key in this regard, first the different scale and secondly the type of reactor. Both aspects can strongly affect the actual numbers shown here, in particular the gasification technology would affect the devolatilization process, due to the different biomass heating profiles as well as the type of contact between the biomass/products and the gasifying agents. Nevertheless the main trends and conclusions can be useful for further evaluation of the integration of torrefaction and gasification processes at the temperature and pressure ranges of the study.

3.2.4.1. H_2/CO and CO/CO_2 ratios in the flue gas. The H_2/CO ratio in the produced gas is important for further possible end uses of the gas. Table 3 shows the evolution of this ratio with the gasification pressure and torrefaction levels of GROT and VW materials, respectively. The ratio ranged between 1.5 and 1.9, but mainly centred in values close to 1.8. These values are quite close to the levels required for methanol or ammonia production or Fischer–Tropsch processes, the latter being the aim of this study for biofuel production [8]. The ratio increased with the torrefaction level whereas the effect of pressure differed depending on the feedstock. Several factors affected the H_2/CO ratio, on the one hand H_2 production increased with torrefaction level and decreased as pressure rises (due to the gasification reactions), on the other hand CO yield also decreased, to a greater or lesser extent depending on the CO/CO_2 equilibrium.

The evolution of CO/CO_2 ratio also appears in Table 3. The value of the ratio was lower than 0.8 in all the studied range, and decreased almost linearly with pressure. The effect of torrefaction was less evident, although a slight increase with the torrefaction level could be observed (more evident in the case of GROT-derived materials).

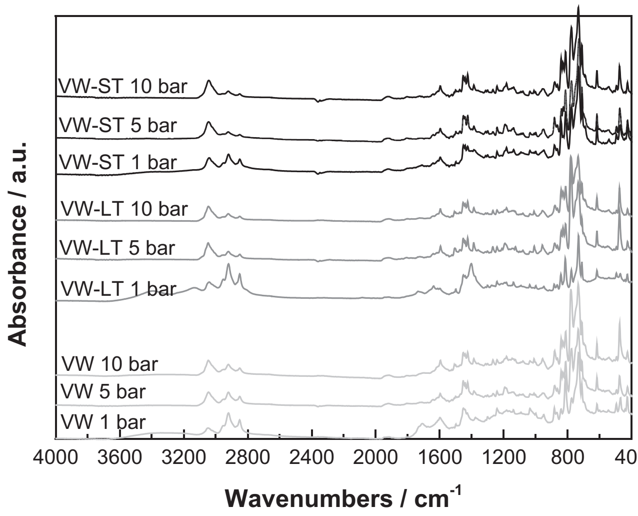

Fig. 9. FTIR spectra of VW tars obtained in an FBR, influence of pressure and torrefaction level.

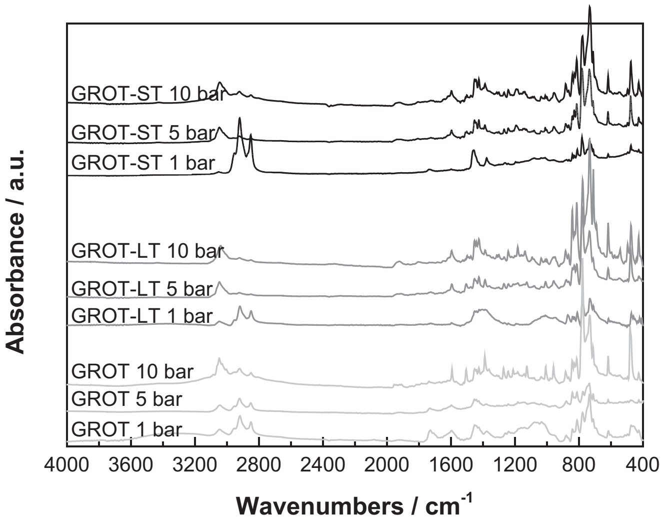

Fig. 10. FTIR spectra of GROT tars obtained in an FBR, influence of pressure and torrefaction level.

3.2.4.2. Carbon conversion. One parameter that gives insight into the performance of gasification process is the conversion of carbon in the gasifier to gaseous products, also known as carbon conversion. This value (see Table 3) was determined as the ratio of carbon leaving the gasifier in the form of gaseous products in the product gas stream to the amount of carbon introduced by the feedstock (Eq. (1)).

$$X_C[\%] = 100\left(\frac{\text{Carbon in producer gas}[\text{kmol/h}]}{\text{Carbon in biomass}[\text{kmol/h}]}\right) \tag{1}$$

The obtained results showed an increase in carbon conversion with gasification pressure in all the studied cases. This fact could be attributed to the higher CO_2 and CH_4 yields obtained under these conditions. The effect of torrefaction on carbon conversion was more significant for the experiments performed on the GROT-derived materials as compared to the analogous VW samples (Table 3). This trend is consistent with the higher tar and char yields obtained in the experiments of GROT materials.

3.2.4.3. Gasifier cold gas efficiency. Another key figure on the gasification performance is the cold gas efficiency (CGE) (Table 3). This parameter is defined as the energy in the gas in relation to energy in the biomass fed (Eq. (2)).

$$CGE_{LHV}[\%] = 100\left(\frac{LHV_{\text{product gas}}[\text{MW}]}{LHV_{\text{biomass}}[\text{MW}]}\right) \tag{2}$$

The calculated CGE values ranged between 60 and 71%, and increased with the gasification pressure in the range from 0.1 to 0.5 MPa, and remained constant or decreased at higher pressures. This trend is in agreement with the higher carbon conversion, however, at higher pressures the lower heating value of the produced gas is related to the higher CO_2 yields, together with the decrease in H_2 yield. Another factor that would influence the CGE in an integrated process is the introduction of the volatiles obtained during the torrefaction process into the gasifier. In this way the efficiency of the global process would improve [31].

Table 3
Influence of experimental conditions on gasification parameters.

Feedstock	Pressure (MPa)	H_2/CO	CO/CO_2	X_C	CGE (LHV)	η_{LHV}
VW	0.1	1.76 ± 0.05	0.74 ± 0.02	88.45 ± 0.45	68.49 ± 0.88	68.49 ± 0.88
VW	0.5	1.75 ± 0.05	0.58 ± 0.01	93.66 ± 0.48	69.73 ± 0.90	69.73 ± 0.90
VW	1.0	1.69 ± 0.05	0.52 ± 0.01	96.68 ± 0.49	69.82 ± 0.90	69.82 ± 0.90
VW-LT	0.1	1.78 ± 0.05	0.76 ± 0.02	89.05 ± 0.46	71.00 ± 0.86	64.81 ± 0.78
VW-LT	0.5	1.68 ± 0.05	0.62 ± 0.02	92.27 ± 0.48	71.36 ± 0.87	65.13 ± 0.79
VW-LT	1.0	1.87 ± 0.05	0.50 ± 0.01	94.75 ± 0.49	70.69 ± 0.85	64.52 ± 0.78
VW-ST	0.1	1.81 ± 0.05	0.76 ± 0.02	83.92 ± 0.43	65.62 ± 0.79	60.61 ± 0.73
VW-ST	0.5	1.79 ± 0.05	0.65 ± 0.02	94.06 ± 0.48	67.24 ± 0.81	62.11 ± 0.75
VW-ST	1.0	1.88 ± 0.05	0.52 ± 0.01	94.60 ± 0.49	67.66 ± 0.82	62.50 ± 0.76
GROT	0.1	1.49 ± 0.04	0.70 ± 0.02	85.12 ± 0.44	59.51 ± 0.73	59.51 ± 0.73
GROT	0.5	1.68 ± 0.05	0.52 ± 0.01	91.90 ± 0.47	67.02 ± 0.82	67.02 ± 0.82
GROT	1.0	1.71 ± 0.05	0.48 ± 0.01	97.35 ± 0.50	69.58 ± 0.85	69.58 ± 0.85
GROT-LT	0.1	1.88 ± 0.05	0.67 ± 0.02	81.71 ± 0.42	64.98 ± 0.78	61.42 ± 0.74
GROT-LT	0.5	1.91 ± 0.05	0.58 ± 0.01	89.13 ± 0.46	70.35 ± 0.84	66.50 ± 0.79
GROT-LT	1.0	1.78 ± 0.05	0.53 ± 0.01	90.84 ± 0.47	68.86 ± 0.83	65.09 ± 0.78
GROT-ST	0.1	1.84 ± 0.05	0.75 ± 0.02	77.98 ± 0.40	62.90 ± 0.75	59.80 ± 0.71
GROT-ST	0.5	1.82 ± 0.05	0.66 ± 0.02	84.96 ± 0.43	67.83 ± 0.81	64.49 ± 0.77
GROT-ST	1.0	1.77 ± 0.05	0.58 ± 0.01	85.42 ± 0.44	65.94 ± 0.79	62.69 ± 0.75

The calculated data also showed that the effect of torrefaction level on CGE was not relevant from the raw material to the lightly torrefied materials, however, a clear decrease in CGE was noticed for the significantly torrefied materials, which could be linked with the lower carbon conversion for the ST materials.

3.2.4.4. Overall torrefaction–gasification efficiency. This parameter is calculated taking into account the energy content of the producer gas in relation to energy content of the raw biomass (previously to the torrefaction process) (Eq. (3)). Fig. 11 presents a diagram that explains the calculation of this parameter.

$$\eta_{LHV}[\%] = 100\left(\frac{\mathrm{LHV}_{\text{product gas}}[\mathrm{MW}]}{\mathrm{LHV}_{\text{raw biomass}}[\mathrm{MW}]}\right) \quad (3)$$

The overall efficiency values ranged between 60 and 69%. These values were lower for torrefied materials than for raw biomass, due to the energy inefficiency related to the loss of volatiles, not used in the process [30]. The results showed an increase of the efficiency with the gasification pressure in the range from 0.1 to 0.5 MPa, and remained constant or decreased at higher pressures. The data also showed a decrease of the global efficiency of the process with the torrefaction level. This reduction is related to both the energy efficiency of the torrefaction process and the lower carbon conversion for the torrefied materials.

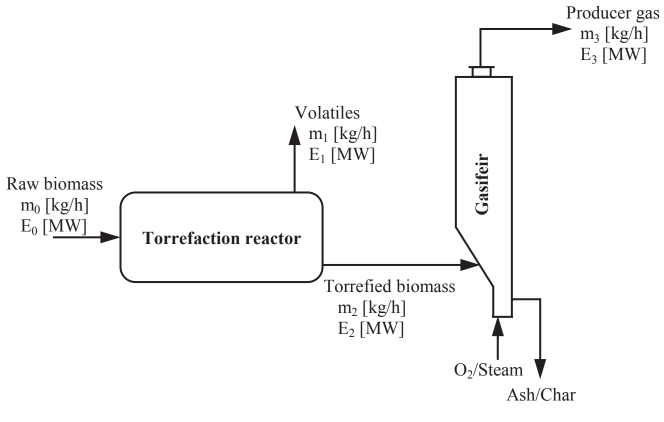

Fig. 11. Schematic diagram of the overall mass and energy balances for the combination of torrefaction and gasification processes.

4. Conclusions

This work reports experimental results concerning the influence of torrefaction level and pressure on product yields and composition during fluidized bed O_2/steam gasification for the production of liquid fuels.

Regarding the torrefaction process, the composition of torrefied samples was closer to that of coal, with higher carbon content and lower volatile matter content, increasing with the torrefaction severity.

Gasification experiments varying pressure and torrefaction level and using two different biomasses were performed in order to determine the effect of these parameters on gasification performance. The main trend for both biomasses was an increase on gas yield with pressure and torrefaction level. Additionally, it was noticed that tar yield increased with the experimental pressure, together with a decrease of char yield.

Pressure made the produced gas composition shift towards higher CH_4 and CO_2 content, while H_2 and CO levels decreased. Regarding the effect of the original biomass, VW-derived materials (VW-LT, VW-ST) yielded higher levels of H_2 and CO, and lower levels of CH_4 than the correspondent GROT-derived materials. The differences became less relevant as pressure and torrefaction level increased (more severe conditions).

The analysis of the obtained tars through SEC and FTIR corroborated that the increase in pressure led to higher tar levels, which could be related to polymerization of the tar compounds towards heavier PAH compounds. Torrefaction level presented the opposite effect, with lower tar yields and lighter molecular weight distribution of tars in the order raw biomass, LT and ST.

This study also provides insight into the influence of pressure and torrefaction level on several key parameters of the gasification performance (H_2/CO and CO/CO_2 Ratios, carbon conversion and cold gas efficiency). The information is of great interest to determine optimal operation conditions. However, an exhaustive evaluation of the different factors is needed for that purpose, as not only technical aspects on thermal conversion or gas composition have to be taken into consideration, but also other factors as the costs associated to the whole process.

Acknowledgements

This research was supported by the European Regional Development Funds (ERDF, “FEDER Programa de Competitivitat de

Catalunya 2007–2013”), the Spanish Government (project CTQ2011-22767, co-funded by the ERDF program), the Norwegian Research Council and a number of industrial partners under the RENERGI Programme (Gasbio: “Gasification for Biofuels”, project no. 199902/S60). C. Berrueco is grateful to the Spanish Ministry of Economy and Competitivity for funding his Ramon y Cajal contract (RYC-2011-09202).

References

[1] Demirbas A. Progress and recent trends in biofuels. Prog Energy Combust Sci 2007;33(1):1–18.
[2] Escobar JC, Lora ES, Venturini OJ, Yáñez EE, Castillo EF, Almazan O. Biofuels: environment, technology and food security. Renew Sustain Energy Rev 2009;13(6–7):1275–87.
[3] Alauddin ZABZ, Lahijani P, Mohammadi M, Mohamed AR. Gasification of lignocellulosic biomass in fluidized beds for renewable energy development: a review. Renew Sustain Energy Rev 2010;14(9):2852–62.
[4] Basu P. Biomass gasification and pyrolysis - practical design and theory. Boston: Academic Press; 2010, ISBN 978-0-12-374988-8.
[5] World energy outlook 2008. International Energy Agency; 2008, ISBN 978-92-64-04560-6.
[6] Re-Thinking 2050. A 100% renewable Energy Vision for the European Union. European Renewable Energy Council; 2010.
[7] Roadmap 2050 – a practical guide to a prosperous low-carbon Europe. European Climate Foundation; 2010.
[8] Higman C, van der Burgt M. In: Gasification. 2nd ed. Burlington: Gulf Professional Publishing; 2008, ISBN 978-0-7506-8528-3.
[9] van der Stelt MJC, Gerhauser H, Kiel JHA, Ptasinski KJ. Biomass upgrading by torrefaction for the production of biofuels: a review. Biomass Bioenergy 2011;35(9):3748–62.
[10] Bach QV, Pfeiffer B, Tran K-Q, Khalil R, Skreiberg Ø. Combustion kinetics of wet-torrefied Norwegian biomass fuels. In: Twentieth European biomass conference and exhibition 2012 – book of proceedings, Milan, Italy; 2012. pp. 1739–44.
[11] Chew JJ, Doshi V. Recent advances in biomass pretreatment – torrefaction fundamentals and technology. Renew Sustain Energy Rev 2011;15(8):4212–22.
[12] Khalil R, Skreiberg Ø. Stable operating conditions in bioenergy plants through utilization of torrefied biomass. In: International Nordic bioenergy 2011 – book of proceedings. Jyväskylä: FINBIO; 2011. pp. 268–71.
[13] Tapasvi D, Khalil R, Skreiberg Ø, Tran K-Q, Grønli M. Torrefaction of Norwegian Birch and Spruce: an experimental study using Macro-TGA. Energy Fuels 2012;26(8):5232–40.
[14] Tapasvi D, Khalil R, Várhegyi G, Skreiberg Ø, Tran K-Q, Grønli M. Kinetic behavior of torrefied biomass in an oxidative environment. Energy Fuels 2013;27(2):1050–60.
[15] Matas Güell B, Sandquist J, Sørum L. Gasification of biomass to second generation biofuels: a review. J Energy Resour Technol Trans ASME 2013;135(1).
[16] El-Emam RS, Dincer I, Naterer GF. Energy and exergy analyses of an integrated SOFC and coal gasification system. Int J Hydrogen Energy 2012;37(2):1689–97.
[17] Gil J, Aznar MP, Caballero MA, Francés E, Corella J. Biomass gasification in fluidized bed at pilot scale with steam–oxygen mixtures. Product distribution for very different operating conditions. Energy Fuels 1997;11(6):1109–18.
[18] Kandiyoti R, Herod A, Bartle K. Solid fuels and heavy hydrocarbon liquids. Oxford: Elsevier Science Ltd; 2006, ISBN 978-0-08-044486-4.
[19] Pereira EG, Da Silva JN, De Oliveira JL, MacHado CS. Sustainable energy: a review of gasification technologies. Renew Sustain Energy Rev 2012;16(7):4753–62.
[20] Lv PM, Xiong ZH, Chang J, Wu CZ, Chen Y, Zhu JX. An experimental study on biomass air–steam gasification in a fluidized bed. Bioresour Technol 2004;95(1):95–101.
[21] González JF, Román S, Bragado D, Calderón M. Investigation on the reactions influencing biomass air and air/steam gasification for hydrogen production. Fuel Process Technol 2008;89(8):764–72.
[22] Gupta AK, Cichonski W. Ultrahigh temperature steam gasification of biomass and solid wastes. Environ Eng Sci 2007;24(8):1179–89.
[23] Kumar A, Eskridge K, Jones DD, Hanna MA. Steam-air fluidized bed gasification of distillers grains: effects of steam to biomass ratio, equivalence ratio and gasification temperature. Bioresour Technol 2009;100(6):2062–8.
[24] Turn S, Kinoshita C, Zhang Z, Ishimura D, Zhou J. An experimental investigation of hydrogen production from biomass gasification. Int J Hydrogen Energy 1998;23(8):641–8.
[25] Mayerhofer M, Mitsakis P, Meng X, de Jong W, Spliethoff H, Gaderer M. Influence of pressure, temperature and steam on tar and gas in allothermal fluidized bed gasification. Fuel 2012;99(0):204–9.
[26] Berrueco C, Venditti S, Morgan TJ, Álvarez P, Millan M, Herod AA, et al. Calibration of size-exclusion chromatography columns with 1-methyl-2-pyrrolidinone (NMP)/chloroform mixtures as eluent: applications to petroleum-derived samples. Energy Fuels 2008;22(5):3265–74.
[27] Herod AA, Bartle KD, Morgan TJ, Kandiyoti R. Analytical methods for characterizing high-mass complex polydisperse hydrocarbon mixtures: an overview. Chem Rev 2012;112(7):3892–923.
[28] Morgan TJ, George A, Alvarez P, Herod AA, Millan M, Kandiyoti R. Isolation of size exclusion chromatography elution-fractions of coal and petroleum-derived samples and analysis by laser desorption mass spectrometry. Energy Fuels 2009;23(12):6003–14.
[29] Chen W-H, Kuo P-C. A study on torrefaction of various biomass materials and its impact on lignocellulosic structure simulated by a thermogravimetry. Energy 2010;35(6):2580–6.
[30] Park S-W, Jang C-H, Baek K-R, Yang J-K. Torrefaction and low-temperature carbonization of woody biomass: evaluation of fuel characteristics of the products. Energy 2012;45(1):676–85.
[31] Prins MJ, Ptasinski KJ, Janssen FJJG. More efficient biomass gasification via torrefaction. Energy 2006;31(15):3458–70.
[32] Deng J, Wang G-j, Kuang J-h, Zhang Y-l, Luo Y-h. Pretreatment of agricultural residues for co-gasification via torrefaction. J Anal Appl Pyrolysis 2009;86(2):331–7.
[33] Bridgeman TG, Jones JM, Shield I, Williams PT. Torrefaction of reed canary grass, wheat straw and willow to enhance solid fuel qualities and combustion properties. Fuel 2008;87(6):844–56.
[34] Prins MJ, Ptasinski KJ, Janssen FJJG. From coal to biomass gasification: comparison of thermodynamic efficiency. Energy 2007;32(7):1248–59.
[35] Boateng AA, Mullen CA. Fast pyrolysis of biomass thermally pretreated by torrefaction. J Anal Appl Pyrolysis 2013;100(0):95–102.
[36] Wannapeera J, Fungtammasan B, Worasuwannarak N. Effects of temperature and holding time during torrefaction on the pyrolysis behaviors of woody biomass. J Anal Appl Pyrolysis 2011;92(1):99–105.
[37] Phanphanich M, Mani S. Impact of torrefaction on the grindability and fuel characteristics of forest biomass. Bioresour Technol 2011;102(2):1246–53.
[38] Berrueco C, Mastral EJ, Esperanza E, Ceamanos J. Production of waxes and tars from the continuous pyrolysis of high density polyethylene. Influence of operation variables. Energy Fuels 2002;16(5):1148–53.
[39] Kern S, Pfeifer C, Hofbauer H. Co-gasification of wood and lignite in a dual fluidized bed gasifier. Energy Fuels 2013;27(2):919–31.
[40] Gómez-Barea A, Ollero P, Leckner B. Optimization of char and tar conversion in fluidized bed biomass gasifiers. Fuel 2013;103(0):42–52.
[41] Knoef HAM, editor. Handbook biomass gasification. The Netherlands: BGT Biomass Technology Group; 2005, ISBN 978-9-08-100681-1.
[42] Kitzler H, Pfeifer C, Hofbauer H. Pressurized gasification of woody biomass – variation of parameter. Fuel Process Technol 2011;92(5):908–14.
[43] Mastral JF, Berrueco C, Ceamanos J. Pyrolysis of high-density polyethylene in free-fall reactors in series. Energy Fuels 2006;20(4):1365–71.
[44] Mastral JF, Berrueco C, Ceamanos J. Theoretical prediction of product distribution of the pyrolysis of high density polyethylene. J Anal Appl Pyrolysis 2007;80(2):427–38.
[45] Richter H, Grieco WJ, Howard JB. Formation mechanism of polycyclic aromatic hydrocarbons and fullerenes in premixed benzene flames. Combust Flame 1999;119(1–2):1–22.